Supplementary Material

An RNA editing/dsRNA binding-independent gene regulatory mechanism of ADARs and its clinical implication in cancer

Lihua Qi[1, 2*], Yangyang Song[1*], Tim Hon Man Chan[1], Henry Yang[1], Chi Ho Lin[3], Daryl Jin Tai Tay[1], HuiQi Hong[1], Szejing Tang[1], Kar Tong Tan[1], Xi Xiao Huang[1], Jaymie Siqi Lin[1], Vanessa Hui En Ng[1], Julien Jean Pierre Maury[4], Daniel G Tenen[1,5], Leilei Chen[1,6]

[1]*Cancer Science Institute of Singapore, National University of Singapore, Singapore;*
[2] *Duke-NUS Medical School, National University of Singapore, Singapore;*
[3]*Centre for Genomic Sciences, the University of Hong Kong;*
[4]*Institute of Molecular and Cell Biology, A*STAR, Singapore;*
[5]*Harvard Stem Cell Institute, Harvard Medical School, Boston, Massachusetts, USA;*
[6]*Department of Anatomy, National University of Singapore, Singapore*
** These authors contributed equally to this work*

Contents:

SUPPLEMENTARY DATA

Selection of target genes undergoing extensive A-to-I editing at 3'UTR sequences

Consistent with previous reports, a global RNA editing analysis revealed that A-to-I editing was significantly enriched in 3'UTRs of spliced mRNA in HCC (Supplementary Fig. S1A) (1). To select genes of high functional importance, we first grouped inferred editing sites at 3'UTRs into 3 groups: NT-specific (N), tumor-specific (T), and common in NT and HCC (N&T), followed by the comparison of editing sites in each group among patients (Supplementary Fig. S1B), which not only assisted in the selection of high-confidence editing targets, as defined by the presence of editing sites in at least 2 out 3 patient samples, but revealed a distinct editing pattern between tumors and the adjacent NT liver tissues (Supplementary Fig. S1C). To experimentally validate our calls, we verified a subset of potential editing sites by performing Sanger sequencing of both DNA and RNA from the same samples that have been utilized for RNA-Seq. Approximately 93% (56/60) of single nucleotide variations (SNVs) were validated as bona fide A-to-I editing (Supplementary Fig. S1D). Considering multiple A-to-I editing sites at 3'UTRs of target genes, their expression correlation with ADARs, and their potential involvement in cancer development, 6 genes {*CCNYL1* (cyclin Y like 1), *TNFAIP8L1* (Tumor Necrosis Factor, Alpha-Induced Protein 8-Like 1), *MDM2* (Mouse double minute 2 homolog), *METTL7A* (Methyltransferase Like 7A), *RBBP9* (retinoblastoma binding protein 9) and *MTDH* (Metadherin)} were selected for further study (Supplementary Table S1).

SUPPLEMENTARY MATERIALS AND METHODS

Analysis of RNA editing

Direct sequencing was performed on PCR products, and the editing frequency was calculated using software ImageJ (http://rsb.info.nih.gov/ij/). The reliability of this method was further verified by cloning of individual sequences as previously described (2). Sequences of the relevant primers are listed in Supplementary Table S3.

Construction of ADARs and mutants

The wild-type ADAR1 (p110) and ADAR2 expression constructs were generated as described previously (2). ADARs DeAminase Domain mutants (referred as DeAD mutants) carry specific point mutations (***ADAR1***: H910Y and E912A; ***ADAR2***: E396A) in the catalytic domain, which could abolish their deaminase activities (3). The dsRNA- binding mutants (referred as EAA mutants) have each of the dsRBD conserved motif mutated from KKXXK to EAXXA by introducing 3 point mutations converting the conserved Lysine (K) to Glutamate (E) or Alanine (A) as previously described (4). All the ADARs mutants used in this study were generated by PCR based mutagenesis (3). Sequences of the cloning primers are listed in Supplementary Table S4.

Construction of Short-hairpin RNAs (shRNAs)

The pLKO.1-puro lentiviral vector was purchased from Sigma-Aldrich®, USA. shRNAs against ADAR1 and METTL7A were designed following instructions of the RNA consortium (http://www.broadinstitute.org/rnai/public/). Selected shRNA sequences are listed in Supplementary Table S5. shRNAs were cloned into PLKO.1-puro vector following Addgene's PLKO.1 protocol (http://www.addgene.org/tools/protocols/plko/). For ADAR2, Validated shRNAs were directly purchased from Sigma-Aldrich® (TRCN0000050939 and TRCN0000050942).

MicroRNA cloning and luciferase screening

Except for miR-27a, microRNA (miRNA) precursors were amplified from human placenta genomic DNA to obtain a fragment containing 500-bp both upstream and downstream of mature miRNAs, and then cloned into the pMIRNA1 lenti-miR expression vector (System Biosciences, CA, USA). Sequences of primers used for cloning the candidate microRNAs are listed in Supplementary Table S6. Since miR-27a localizes in a miRNA cluster miR-23a-27a-

24-2, only the pre-miRNA sequence was cloned into pMIRNA1 vector due to its close proximity to other miRNAs in the same cluster. Co-transfection of pMIRNA1-miRNAs with pmirGLO-*METTL7A*-3'UTR was performed in HEK293T cells at a mass ratio of 9:1 to screen for miRNAs which could directly target *METTL7A* 3'UTR, followed by the detection of luciferase activity 48 hours post the co-transfection. In order to confirm the targeting of miR-27a against the *METTL7A* 3'UTR, a dose-dependent assay was conducted with a mass ratio of pMIRNA1-miR-27a to pmirGLO-*METTL7A*-3'UTR ranging from 1: 0.4, 1:0.8, and 1: 1.6. Results were presented as relative firefly luciferase activity after normalization to internal control renilla luciferase and pmirGLO empty vector alone control.

RNA preparation and quantitative real-time PCR (qRT-PCR)

Total RNA was prepared from each sample using the RNeasy mini kit (Qiagen, Hilden, Germany). For miRNA expression analysis, total RNA from Huh-7 cells was prepared using the mirVana™ miRNA Isolation Kit (Life Technologies, CA, USA). Reverse transcription was performed with 500 ng of total RNA and SuperScript® III Reverse Transcriptase (Life Technologies, CA, USA). QRT-PCR was performed with GoTaq® qPCR Master Mix (Promega, USA) using a Rotor-Gene 6000 (Qiagen, Germany). For miRNA expression analysis, 10 ng of total RNA and 0.5 µL of synthetic RNA spike-in (5×10^7 copies) were reverse transcribed with miRCURY LNA™ Universal RT microRNA PCR reagents (Exiqon, Vedbaek, Denmark). Complementary DNA (cDNA) was diluted 20 times, and quantification of miRNAs was performed using the diluted cDNA with ExiLENT SYBR® Green Master Mix Kit (Exiqon, Denmark). Individual miRNA LNA™ PCR primer sets were also purchased from Exiqon. To detect the expression of pre-miR-27a, we conducted a TaqMan® gene expression assay consisting of a pair of unlabelled PCR primers and a TaqMan® probe with a FAM™ label on the 5' end, and minor groove binder (MGB) on the 3' end. Quantification of pre-miRNAs was performed using the diluted cDNA with TaqMan® Gene Expression Master Mix (Applied Biosystems, California, USA). All qRT-PCR primers and probe are listed in Supplementary Table S7.

Western blot analysis

Protein lysates were quantified and resolved on an SDS-PAGE gel, transferred onto a polyvinylidene difluoride (PVDF) membrane (Millipore, Billerica, MA, USA) and immunoblotted with a primary antibody followed by incubation with a secondary antibody. The blots were visualized by enhanced chemiluminescence (GE Healthcare,

Buckinghamshire, UK). The following antibodies were used: antibodies to METTL7A (1:50, Santa Cruz Biotechnology, sc-130168), Dicer (1:1,000, Abcam, ab14601), FLAG (1:2,000, Abcam, ab125243), ADAR1 (1:1,000, Abcam, ab88574), ADAR2 (1:500, Sigma-Aldrich, SAB1405426), Actin (1:5,000, Abcam, ab6276), Fibrillarin (1:1,000, Abcam, ab4566), Lamin A/C (1:1,000, Abcam, ab40567) and α-tubulin (1:1,000, Santa Cruz Biotechnology, sc-5286). The ImageJ program (available at http://rsb.info.nih.gov/ij/) was used for densitometric analyses of western blots, and the quantification results were normalized to the loading control.

Northern blotting analysis for miRNA

Total RNAs were isolated from Huh-7 cells that were transfected with empty vector (EV) or different ADARs expression constructs including the wild-type and EAA mutants. Total RNAs (30 μg) were run on 15% (wt/vol) polyacrylamide–urea gels. Subsequently, RNAs were transferred by electroblotting onto Hybond N+ membrane (Amersham Pharmacia Biotech, Piscataway, NJ) and hybridized with ^{32}P end-labeled miR-27a probe (GCGGAACTTAGCCACTGTGAA, Exiqon, MA, USA) using T4 Polynucleotide Kinase (T4 PNK). After thorough washing, membrane was exposed to an X-ray film at -80˚C overnight.

***In vitro* cell proliferation assay**

1×10^3 cells were seeded per well in a 96-well plate. A 50μL volume of the XTT working solution provided by the kit (Roche Diagnostics, IN, USA) was added to each well. The cells were incubated at 37°C in the dark for 4 hr, followed by the detection of the absorbency using a scanning multi-well spectrophotometer (Tecan Sunrise, Tecan Trading AG, Switzerland) at a test wavelength of 490 nm and a reference wavelength of 630 nm. The data are expressed as the mean ± s.e.m. of triplicate wells within the same experiment. Three independent experiments were conducted.

Foci formation and colony formation in soft agar assays

For the foci formation assay, 1×10^3 cells were seeded in a 6-well plate. After culture for 7 days, surviving colonies (>50 cells per colony) were counted and stained using crystal violet (Sigma-Aldrich), and the data were expressed as the mean ± s.e.m. of triplicate wells within the same experiment. Triplicate independent experiments were performed.

For colony formation in soft agar, 5×10^3 cells in 0.4% bacto agar were seeded on top of a solidified layer of 0.6% bacto agar in 6-well plates. Colonies consisting of more than 50 cells were counted after 3 weeks, and the data were expressed as the mean ± s.e.m. of triplicate wells within the same experiment. Triplicate independent experiments were performed.

***In vivo* tumorigenicity assay**

Briefly, 200 μL of mixture of matrigel and RPMI /DMEM (1:1) containing 3×10^6 of control or *METTL7A*-overexpressing or –knockdown cells were injected subcutaneously into the left and right flanks of a 4- to 5-week old male NOD/SCID mouse, respectively. Tumor formation was monitored for 3 weeks, and tumor volume was measured and calculated by the formula Volume = 0.5 × width × width × length. All mice were kept on a standard chow diet and had free access to food and water. All experiments were approved by Institutional Animal Care and Use Committee (IACUC) of National University of Singapore (NUS) (IACUC protocol No. R12-4194).

SUPPLEMENTARY LEGENDS TO FIGURES

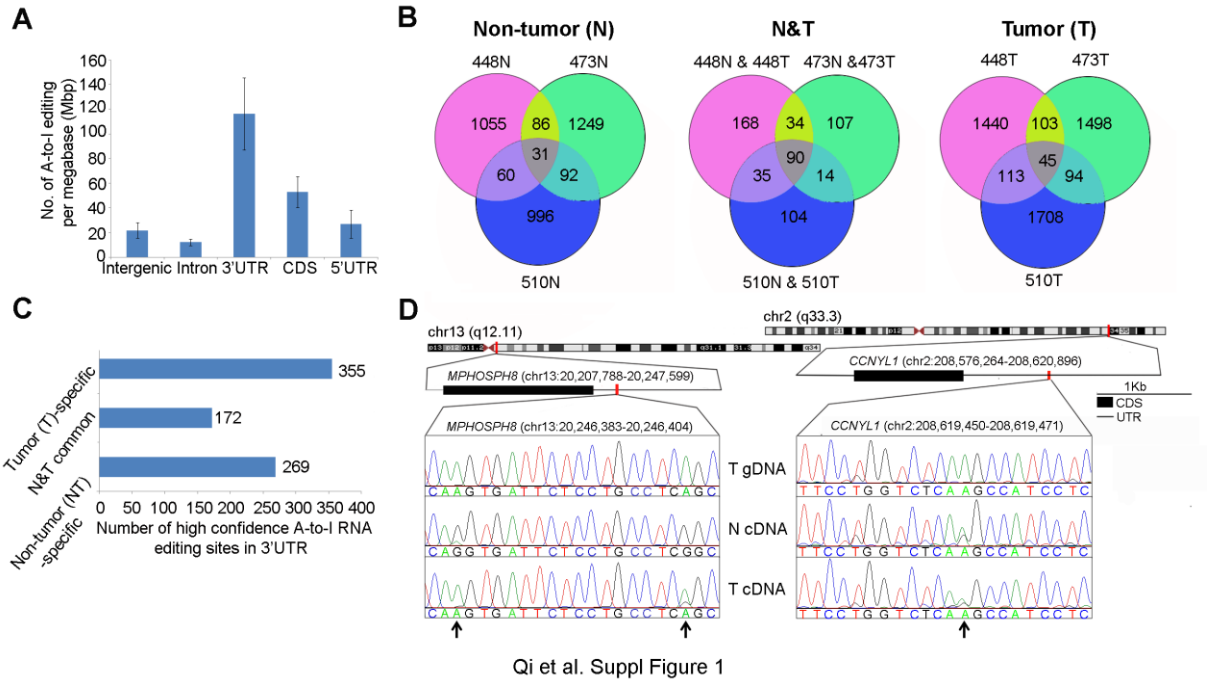

Figure S1. Selection of target genes undergoing extensive A-to-I editing at 3'UTR sequences. (**A**) Distribution of the potential editing sites across different genetic elements in HCC, calculated based on the incidence per unit length (Mbp, mega-base pairs) from the RNA-sequencing (RNA-Seq) datasets (1, 2). (**B**) Intersection of potential 3'UTR editing sites among 3 patients (Case No. 448, 473 and 510). The high-confidence 3'UTR editing sites were categorized into N, N&T, and T groups for each patient sample based on their presence in the adjacent NT or/and HCC tumor tissues. (**C**) Bar chart represents the number of 3'UTR editing sites (**B**) that are present in at least 2 patients of each group. (**D**) Validation of the inferred A-to-I editing sites by Sanger sequencing. Sequence chromatograms of 3 editing sites in 2 genes *MPHOSPH8* and *CCNYL1* (editing sites are indicated by arrows). The complementary DNA (cDNA) samples of one matched pair of tumor (T cDNA) and adjacent NT liver specimens (N cDNA) as well as genomic DNA extracted from the tumor tissue (T gDNA) were included for sequencing.

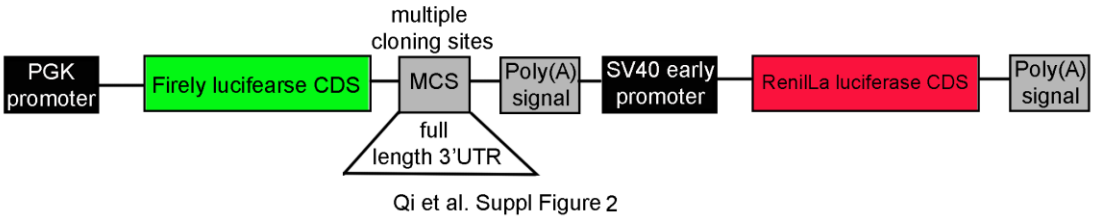

Figure S2. Schematic diagram of pmirGLO Dual-Luciferase expression vector. The full-length 3'UTR sequences of selected genes were cloned into the multiple cloning site (MCS).

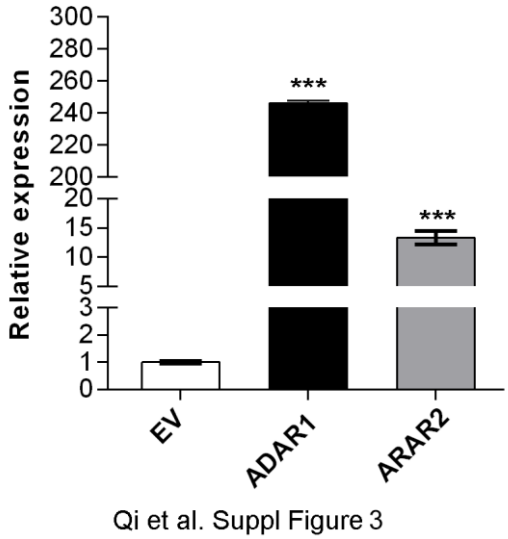

Figure S3. Overexpression of ADARs in HEK293T cells. Real-time quantitative PCR (qRT-PCR) analyses of *ADAR1* and *ADAR2* (ADARs) expression in HEK293T cells. Data are presented as the mean ± s.e.m. of triplicates from a single experiment and representative of 3 independent experiments (***, $P < 0.001$). Statistical significance was determined by unpaired, two-tailed Student's *t* test.

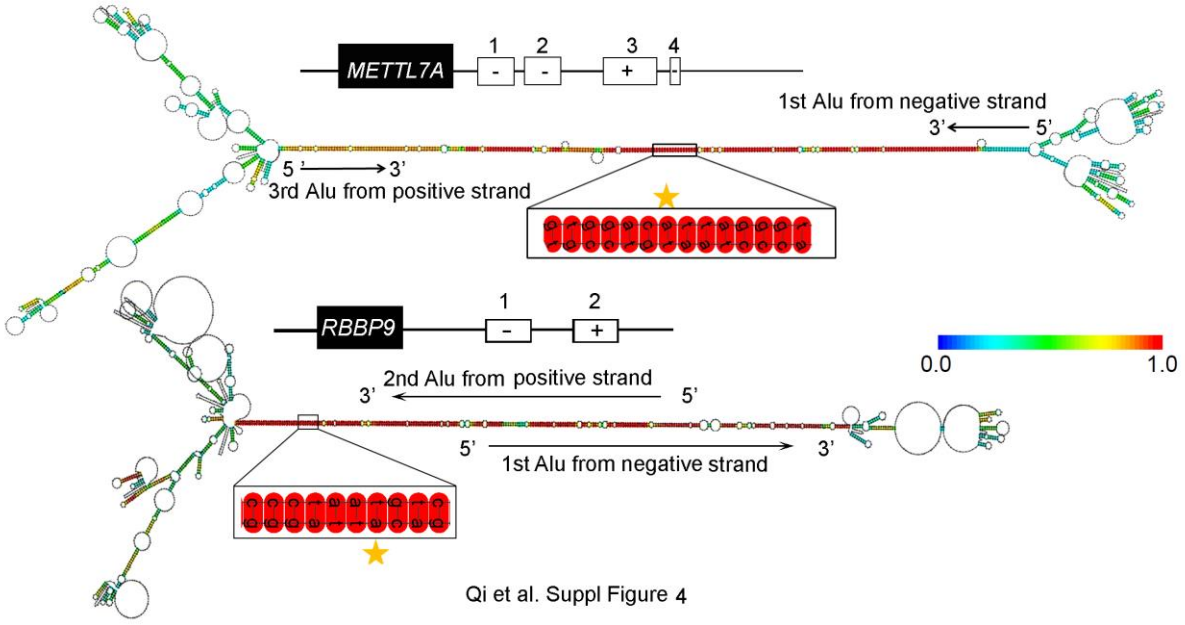

Figure S4. The predicted dsRNA structures of the *METTL7A* and *RBBP9* 3'UTRs. The 3'UTR sequence of *METTL7A* is predicted to form long dsRNA secondary structures between the first *Alu* element on the negative DNA strand and the third *Alu* element on the positive DNA strand using *CentroidFold* (5), spanning approximately 300-bp. The predicted dsRNA structure was also found to be formed from a sense *Alu* and an antisense *Alu* repeats at the 3'UTR sequence of *RBBP9* gene. The heat colour gradation from blue to red indicates base-pairing possibility from 0 to 1. The magnified view shows the partial sequence of the predicted dsRNA with one editing site (indicated by the asterisk).

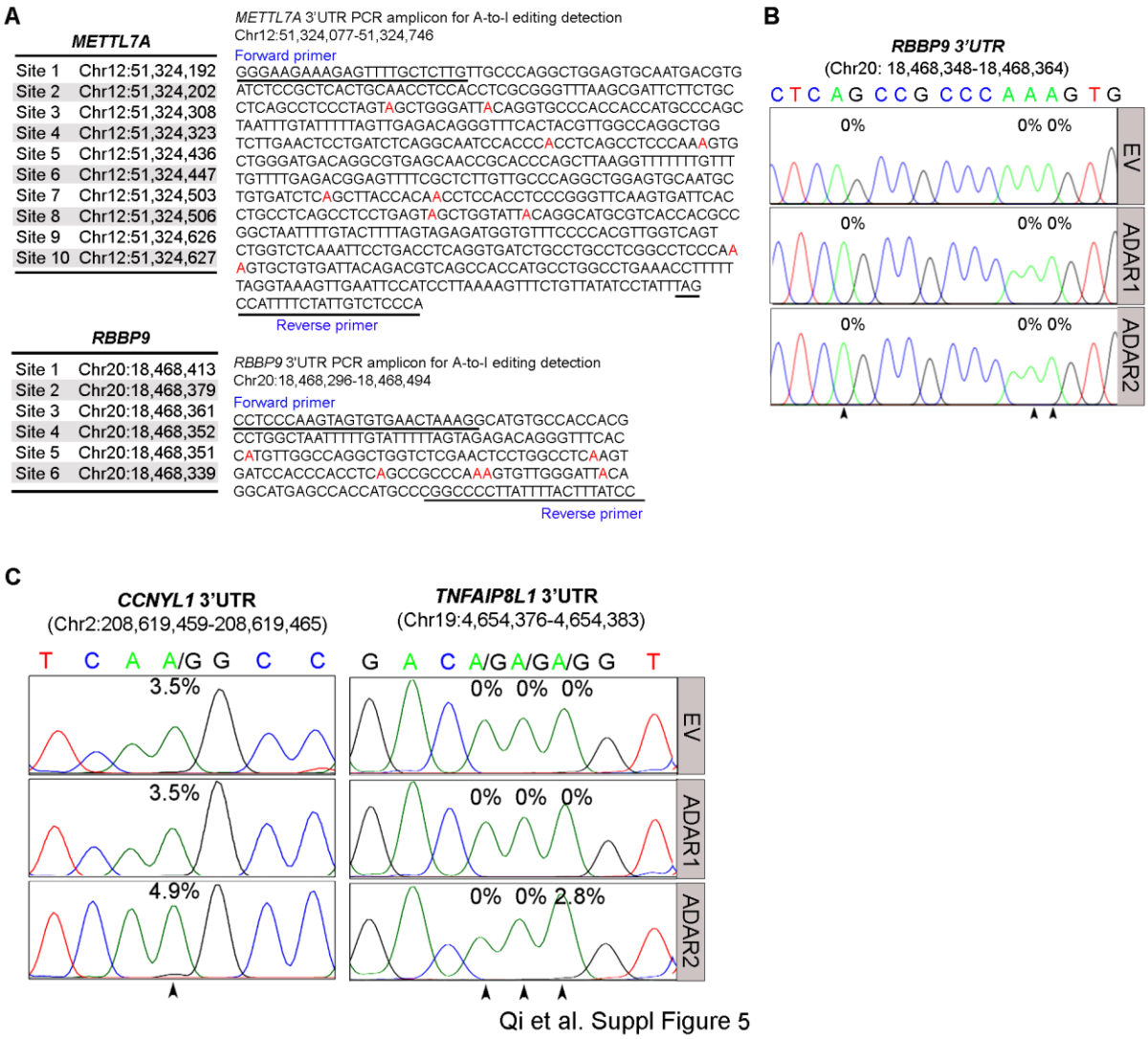

Figure S5. The effect of ADARs on editing levels of multiple sites at 3'UTRs of target genes. (**A**) Tables showing the genomic loci of multiple editing sites in *METTL7A* and *RBBP9* 3'UTRs. The sequences of forward and reverse primers used for PCR amplification are underlined, and editing sites are highlighted in red. (**B**) Sequence chromatograms of 3 editing sites at RBBP9 3'UTR measured 48 hours post co-transfection with 64 ng of EV, ADAR1 or ADAR2 expression construct into HEK293T cells as described in Fig. S3. EV, empty vector. (**C**) Sequence chromatograms of *CCNYL1* and *TNFAIP8L1* 3'UTRs upon *ADAR1* or *ADAR2* overexpression as described in Figure 1B. Percentages denote the editing frequencies of the corresponding editing sites indicated by arrowheads (B, C).

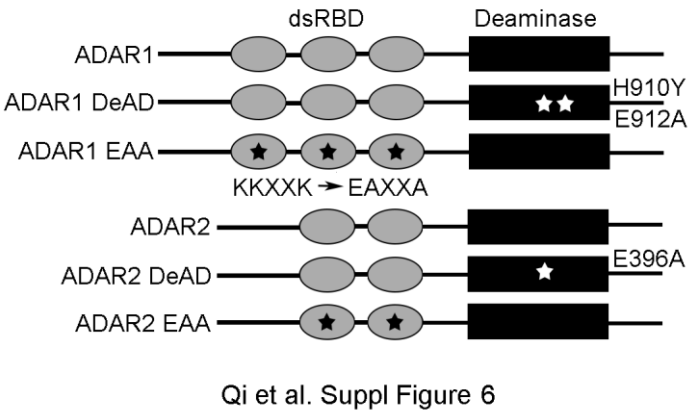

Figure S6. Schematic diagram of different ADARs mutants. ADARs DeAD mutants (DeAmianse Domain mutants) carry point mutations in the deaminase domain to abolish ADARs' deaminase activities (H910Y|E912A for ADAR1, and E396A for ADAR2)(3), while ADARs EAA mutants (dsRNA binding-depleted mutants) harbour mutation of KKXXK to EAXXA in all dsRNA binding domains (dsRBDs) (4).

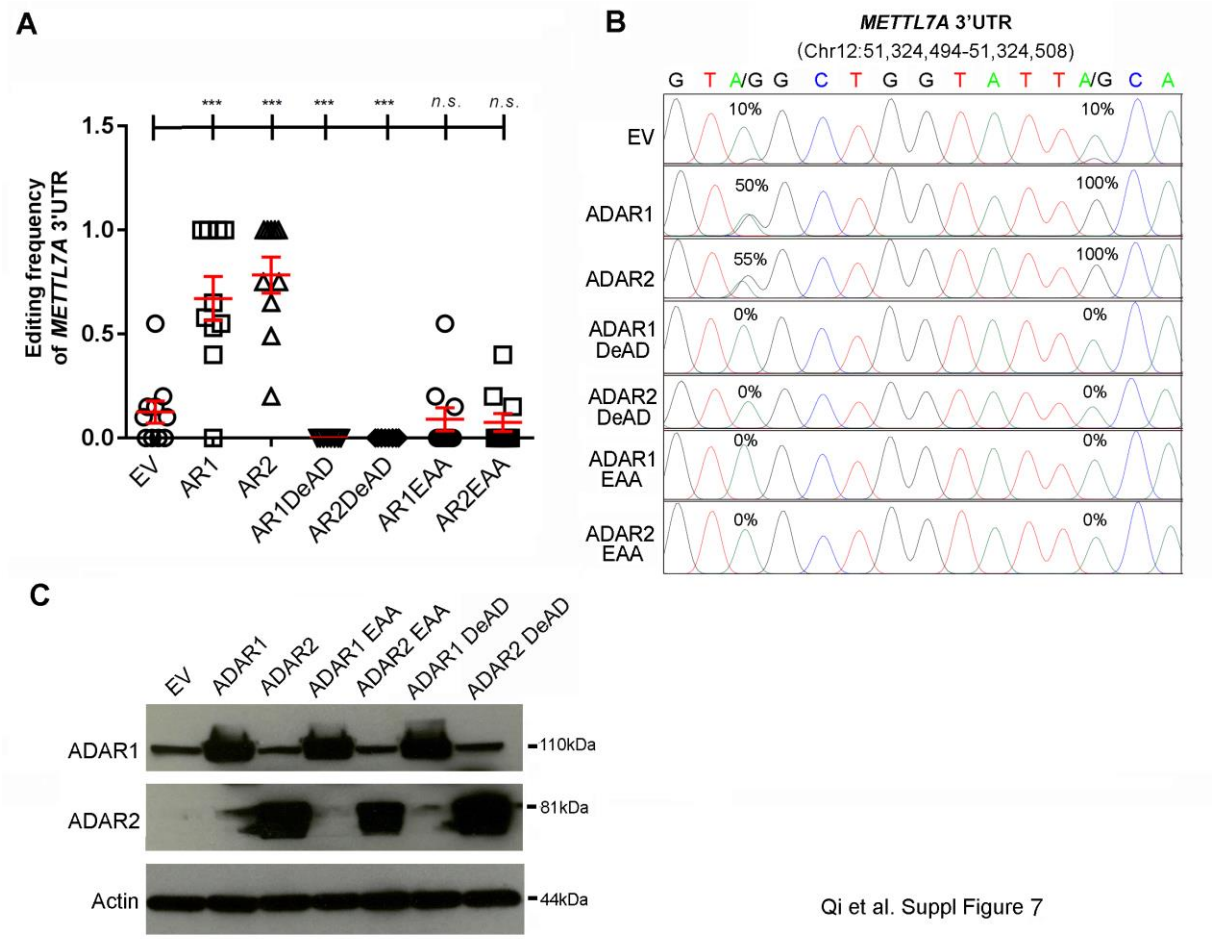

Figure S7. The effects of different forms of ADARs on exogenous *METTL7A* 3' UTR. (**A**) Scatter plots showing the editing frequencies of 10 editing sites at 3' UTR of exogenous *METTL7A* transcripts that were introduced into HEK293T cells by the luciferase reporter vector, upon overexpression of different ADARs. The data are presented with median (horizontal line) and interquartile range (error bar) for each group (Mann–Whitney U test; ***, $P < 0.001$; n.s., not significant). (**B**) Sequence chromatograms of 2 representative editing sites within *METTL7A* 3'UTR. Percentages denote the editing frequencies of the corresponding editing sites. (**C**) Western blot analyses of the indicated proteins in HEK293T cells 48 hours after transfection with the wild-type, DeAD or EAA mutants of ADARs.

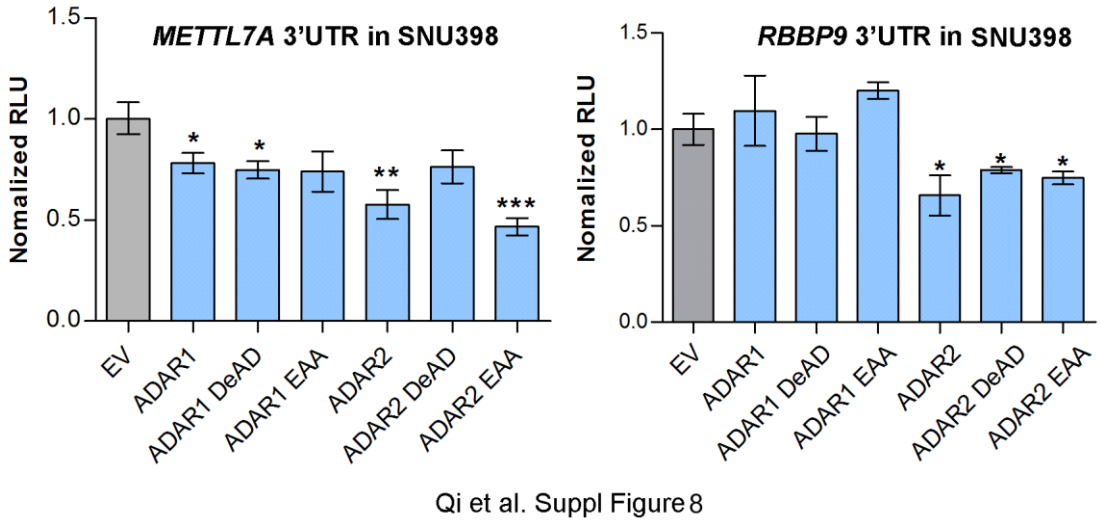

Figure S8. Suppression of ADARs on the expression of target gene *METTL7A* and *RBBP9* in HCC cells. Luciferase activity of pmirGLO-*METTL7A*-3'UTR or pmirGLO-*RBBP9*-3'UTR 48 hours post co-transfection with the control EV or different ADARs (wild-type and mutants) in SNU-398 cells. Data are presented as the mean ± s.e.m. of 6 replicates from a single experiment and representative of 3 independent experiments (*, $P < 0.05$; **, $P < 0.01$; ***, $P<0.001$). Statistical significance was determined by unpaired, two-tailed Student's *t* test.

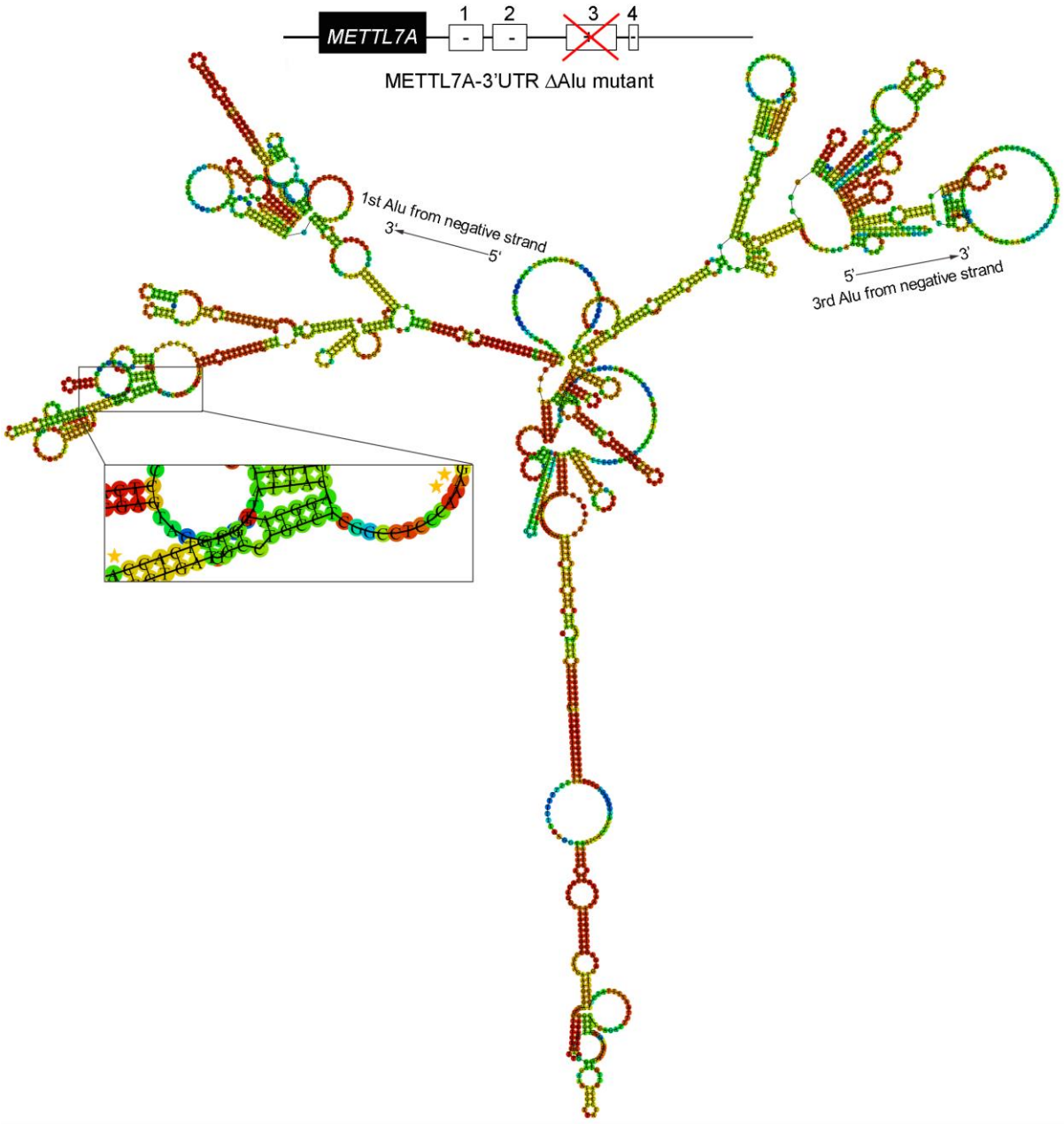

Figure S9. The predicted dsRNA structures of the ΔAlu mutant of *METTL7A* 3'UTRs. The long dsRNA secondary structure is destroyed in the third *Alu*-depleted mutant of *METTL7A* 3'UTR (ΔAlu), as predicted by *CentroidFold*. The heat colour gradation from blue to red indicates base-pairing possibility from 0 to 1. The magnified view shows the partial sequence with three editing sites (indicated by the asterisk).

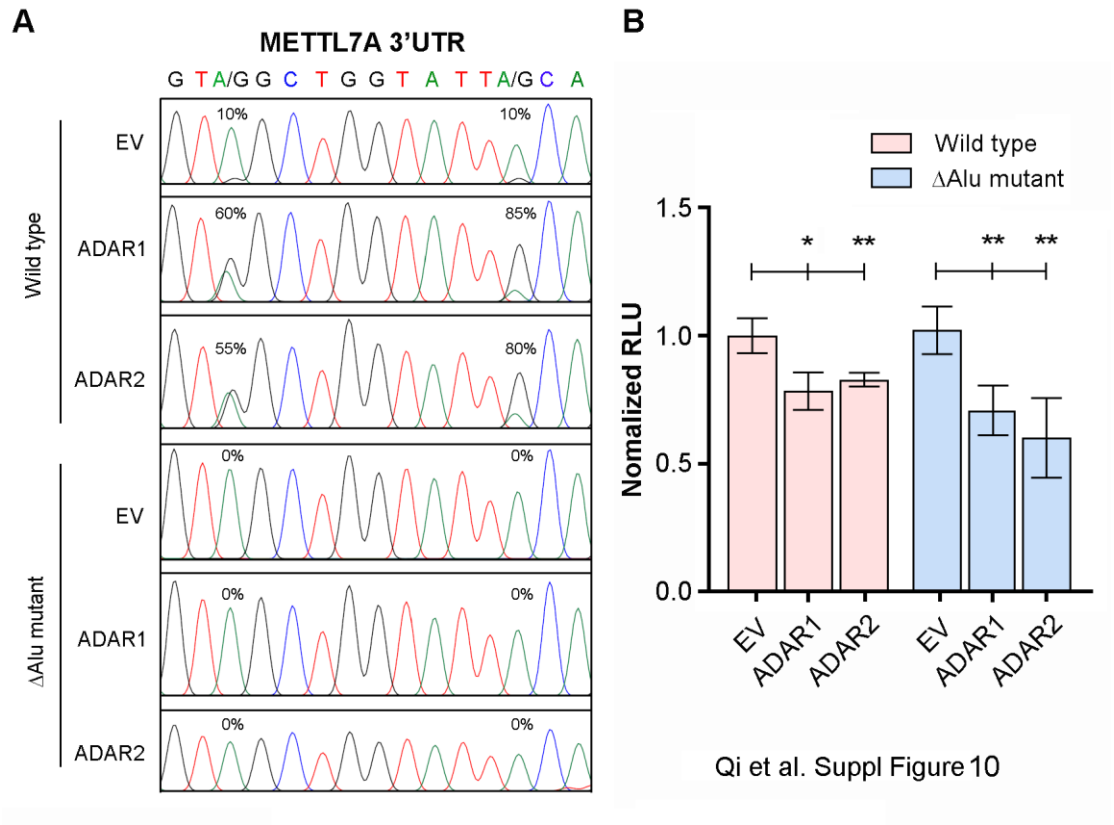

Figure S10. The change in METTL7A expression caused by ADARs is not attributed to the editing of *METTL7A* 3'UTRs. **(A)** Sequence chromatograms of 2 representative editing sites within the wild-type *METTL7A* 3'UTR and ΔAlu mutant upon the overexpression of ADARs. **(B)** Luciferase activity of pmirGLO-METTL7A-3'UTR and pmirGLO- METTL7A 3'UTR (ΔAlu) 48 hours post co-transfection with the control empty vector (EV) or different ADARs constructs in HEK293T cells. Data are presented as the mean ± s.e.m. of 6 replicates from a single experiment and representative of 3 independent experiments (*, $P < 0.05$; **, $P < 0.01$). Statistical significance was determined by unpaired, two-tailed Student's *t* test.

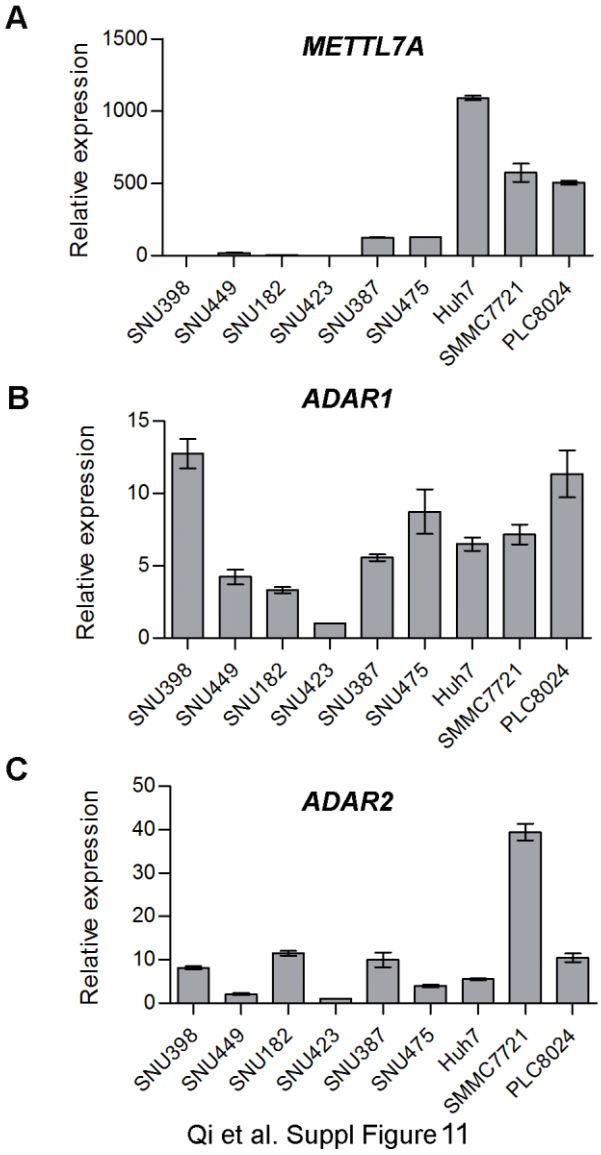

Figure S11. The mRNA expression levels of *METTL7A*, *ADAR1* and *ADAR2* in HCC cells lines. The qRT-PCR detection of *METTL7A* (**A**), *ADAR1* (**B**) and *ADAR2* (**C**) across 9 HCC cell lines. Data are presented as the mean ± s.e.m. of triplicates from a single experiment and representative of 3 independent experiments.

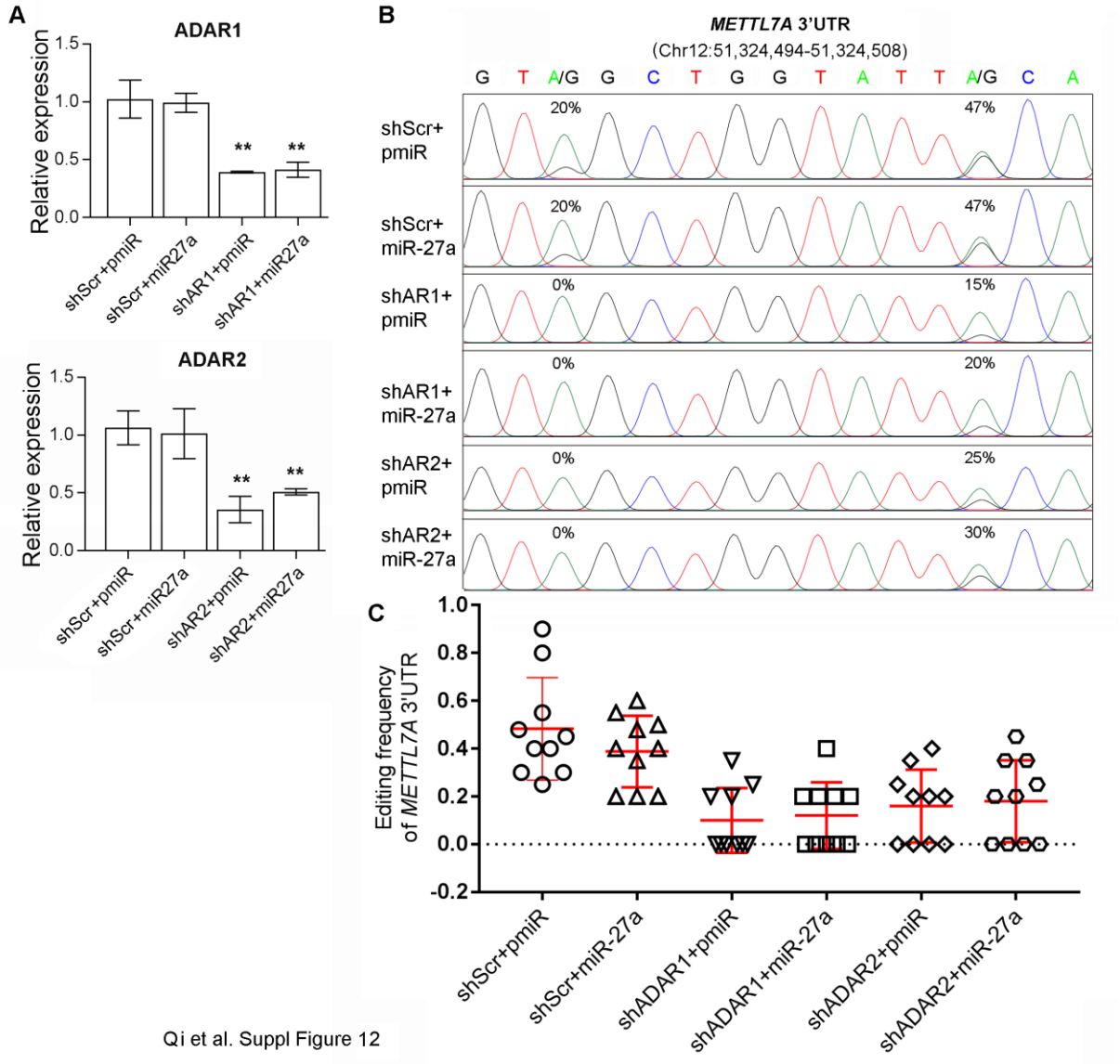

Figure S12. MiR-27a as a mediator between ADARs and METTL7A. (**A**) The qRT-PCR measurement of ADAR1/2 in SMMC7721 cells that were co-transfected with shRNA against *ADAR1* (shADAR1_a), *ADAR2* (shADAR2_a) or scrambled shRNA (shScr) and pMIRNA1-miR-27a (miR-27a) or pMIRNA1 only (pmiR). (**B**) Sequence chromatograms of 2 representative editing sites within *METTL7A* 3'UTR in the indicated cells. Percentages denote the editing frequencies of the corresponding editing sites. (**C**) Scatter plots showing editing frequencies of 10 editing sites at *METTL7A* 3'UTR. The data are presented with median (horizontal line) and interquartile range (error bar) for each group of cells.

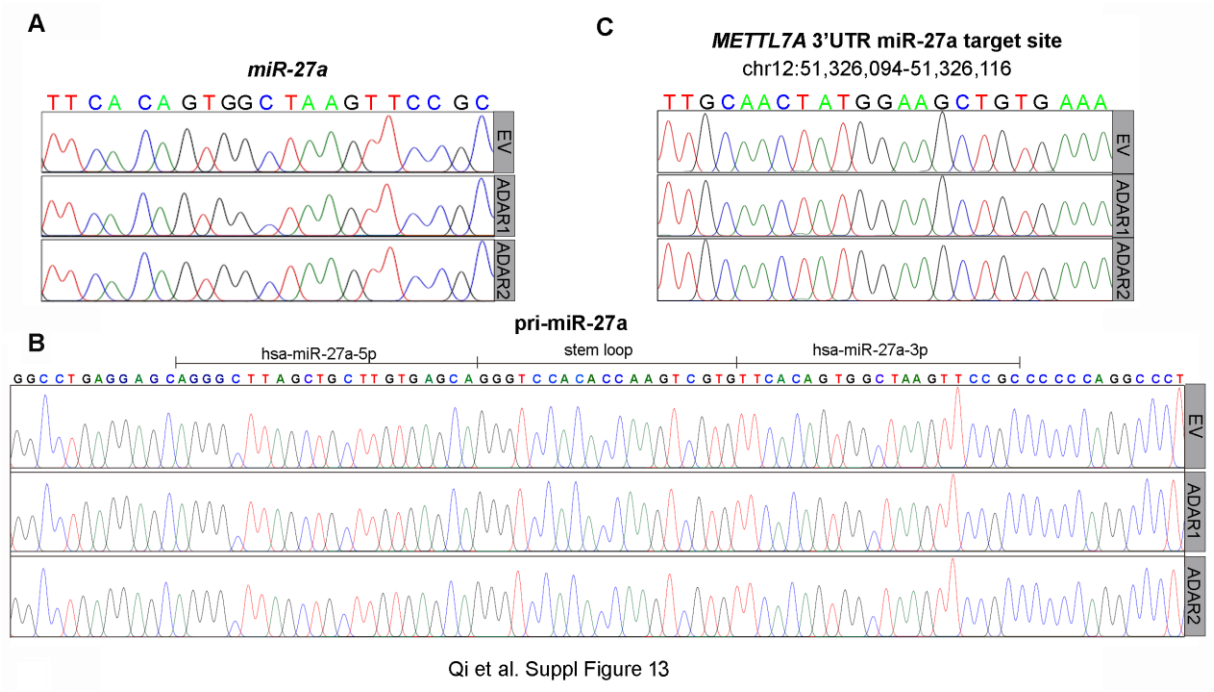

Figure S13. No editing in pri-miR-27a, miR-27a and miR-27a target sequence within the *METTL7A* 3' UTR. (**A-C**) Sequence chromatograms of mature miR-27a (**A**), primary miR-27a (pri-miR-27a) (**B**) and the predicted *METTL7A* 3'UTR sequence targeted by miR-27a (**C**), in Huh-7 cells overexpressing ADAR1, ADAR2 or empty control (EV).

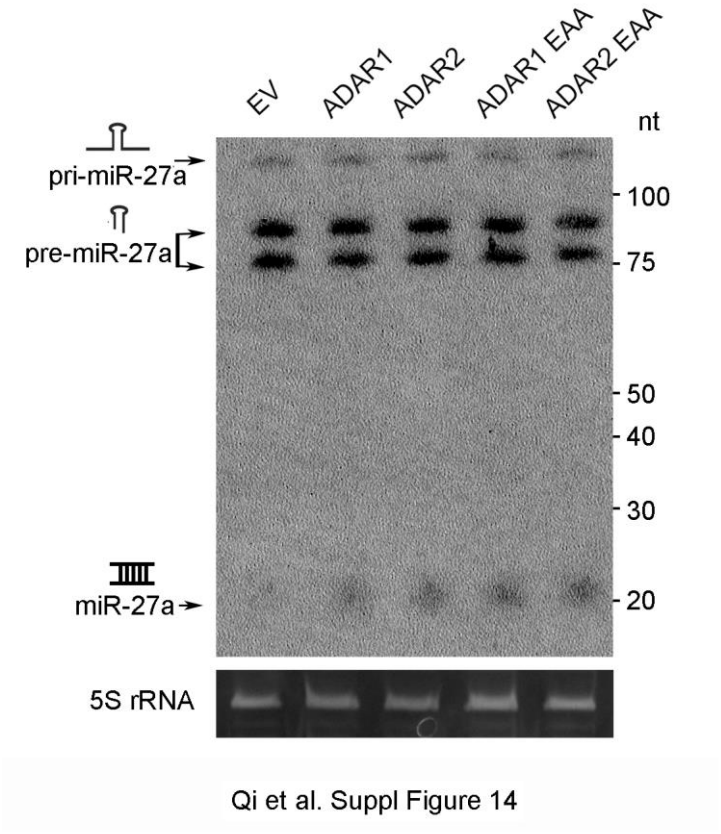

Figure S14. ADARs enhance the processing of pre-miR-27a to mature miR-27a independent of RNA editing/dsRNA binding activities. Northern blot analysis of mature miR-27a, pri-miR-27a, and pre-miR-27a in in Huh-7 cells upon overexpression of empty vector (EV) or different ADARs expression constructs including the wild-type and EAA mutants. 5S rRNA bands stained with ethidium bromide are presented as a loading control.

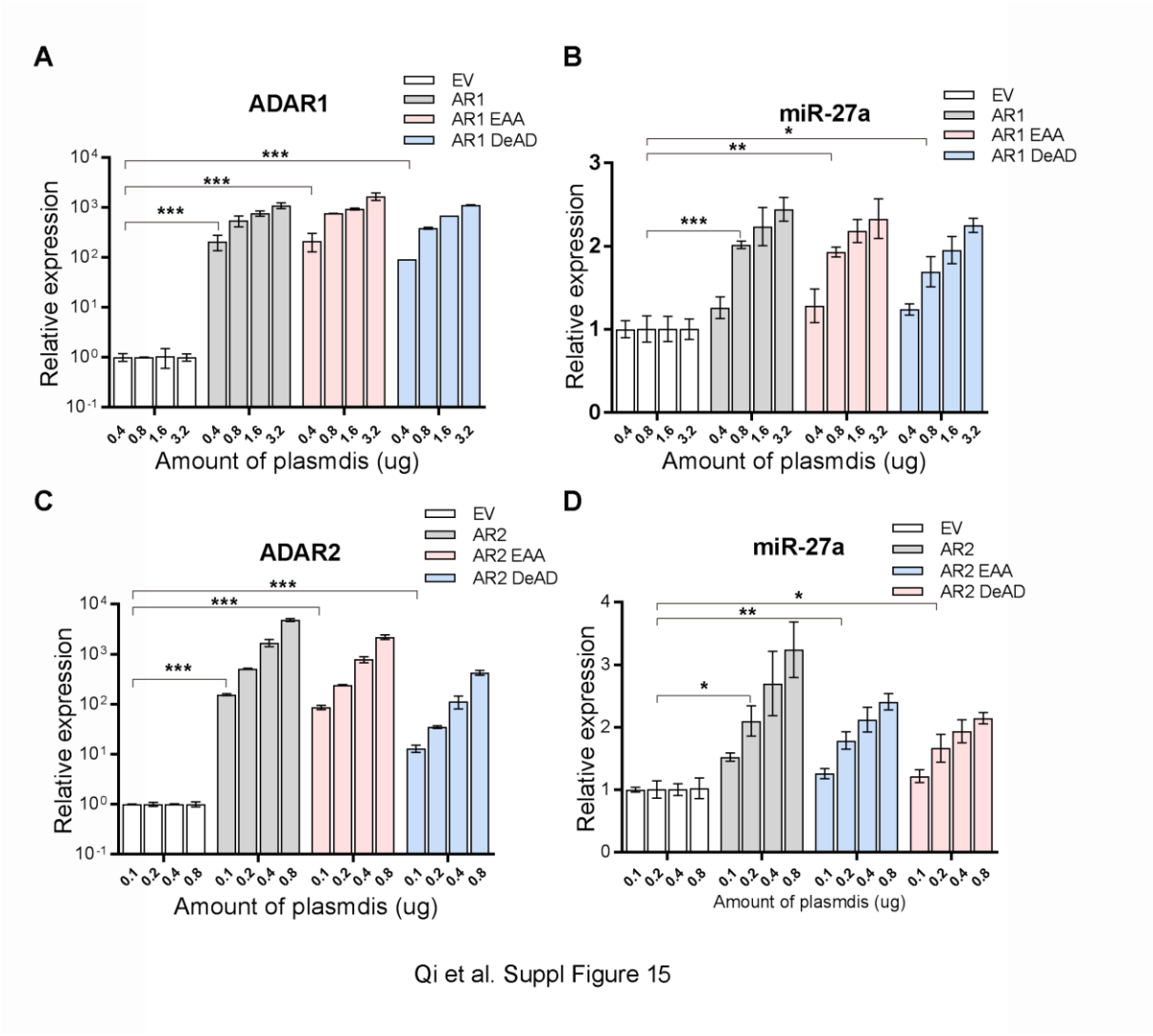

Figure S15. ADARs enhance miR-27a expression independent of RNA editing/dsRNA binding activities. HEK293T cells were seeded in 6-well plates and transfected with the wild-type, DeAD, or EAA forms of ADAR1/2 into cells in a dose-dependent manner with the plasmid DNA amount ranging from 0.4 μg to 3.2 μg (**A**, for each form of *ADAR1*) or 0.1 μg to 0.8 μg (**C**, for each form of *ADAR2*), followed by the detection of mature miR-27a expression (**B**, **D**) in the indicated groups of cells. Data are presented as the mean ± s.e.m. of 6 replicates from a single experiment and representative of 3 independent experiments. Statistical significance was determined by unpaired, two-tailed Student's *t* test. (*, $P < 0.05$; **, $P < 0.01$; ***, $P < 0.001$).

Figure S16. ADARs interact with Dicer in Huh-7 cells. Reciprocal IP of endogenous ADARs and Dicer was conducted in Huh-7 cells using an ADAR1, ADAR2 or Dicer-specific antibody (IP: ADAR1, ADAR2 or Dicer) or mouse IgG (IP: IgG). Western blot analyses of the indicated proteins in ADAR1, ADAR2, Dicer or mouse IgG-IPed products were conducted. Input indicates 5% of whole-cell lysates from Huh-7 cells.

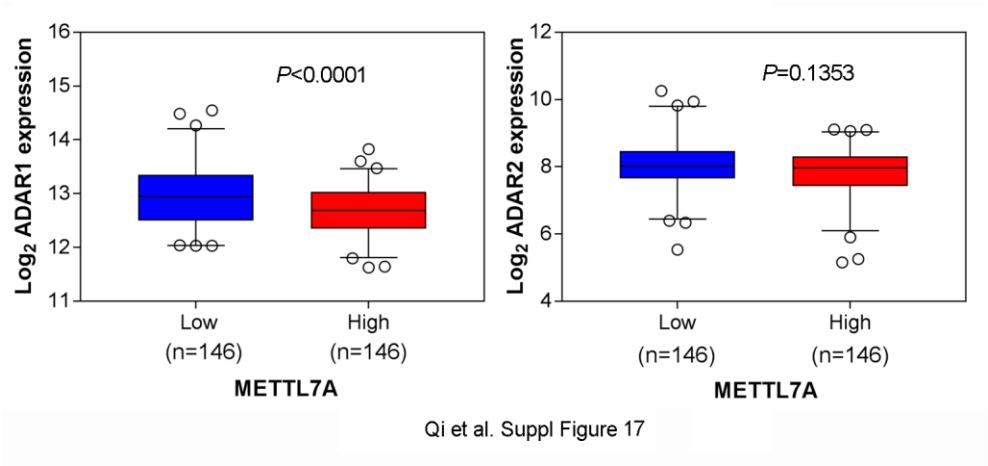

Figure S17. Expression level of METTL7A is decreased in HCC patients demonstrating higher expression of ADARs. Box plots showing the expression level of either ADAR1 (left panel) or ADAR2 (right panel) in METTL7A-high and METTL7A-low groups of patients, based on the TCGA RNA-Seq dataset. The data are presented as box plots with median (horizontal line), 2.5–97.5% (box) and 5–95% (error bar) percentiles for each group and the open dots indicate the outliers (Mann–Whitney U test).

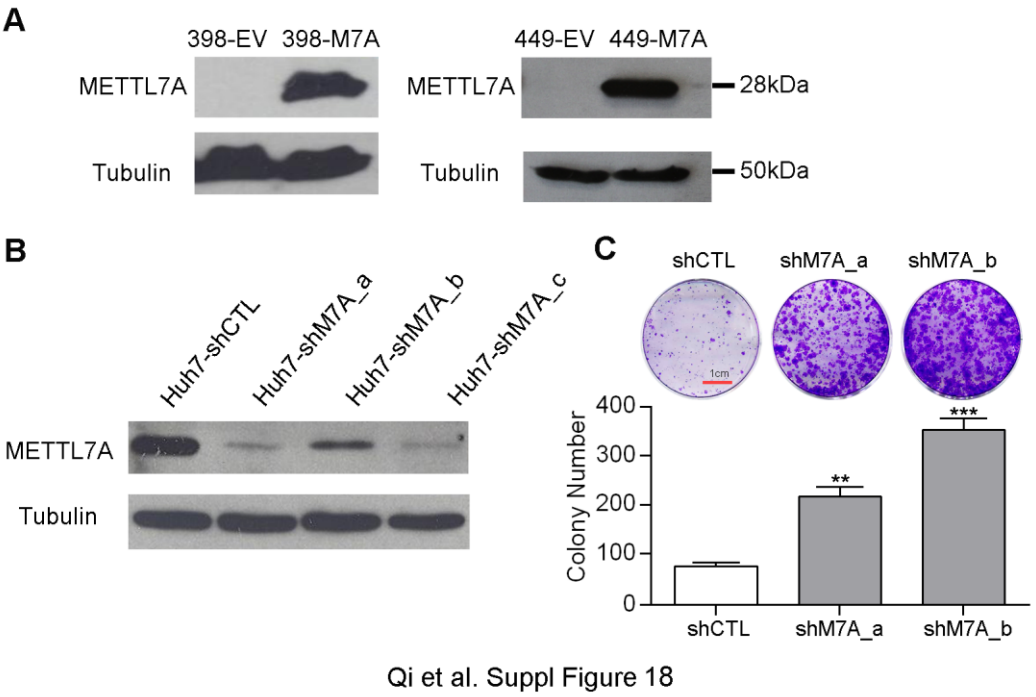

Figure S18. *METTL7A* is a novel tumor suppressor in HCC. *METTL7A* is a novel tumor suppressor in HCC. (**A, B**) Western blot analysis of METTL7A protein in the indicated cell lines. Tubulin was the loading control. (**C**) Quantification of foci formation induced by the stably knockdown cell lines (**, $P < 0.01$; ***, $P < 0.001$). All data are shown as the mean ± s.e.m. of triplicate wells with the same experiment and representative of 3 independent experiments, and statistical significance was determined by unpaired, two-tailed Student's *t* test. Scale bar, 1cm.

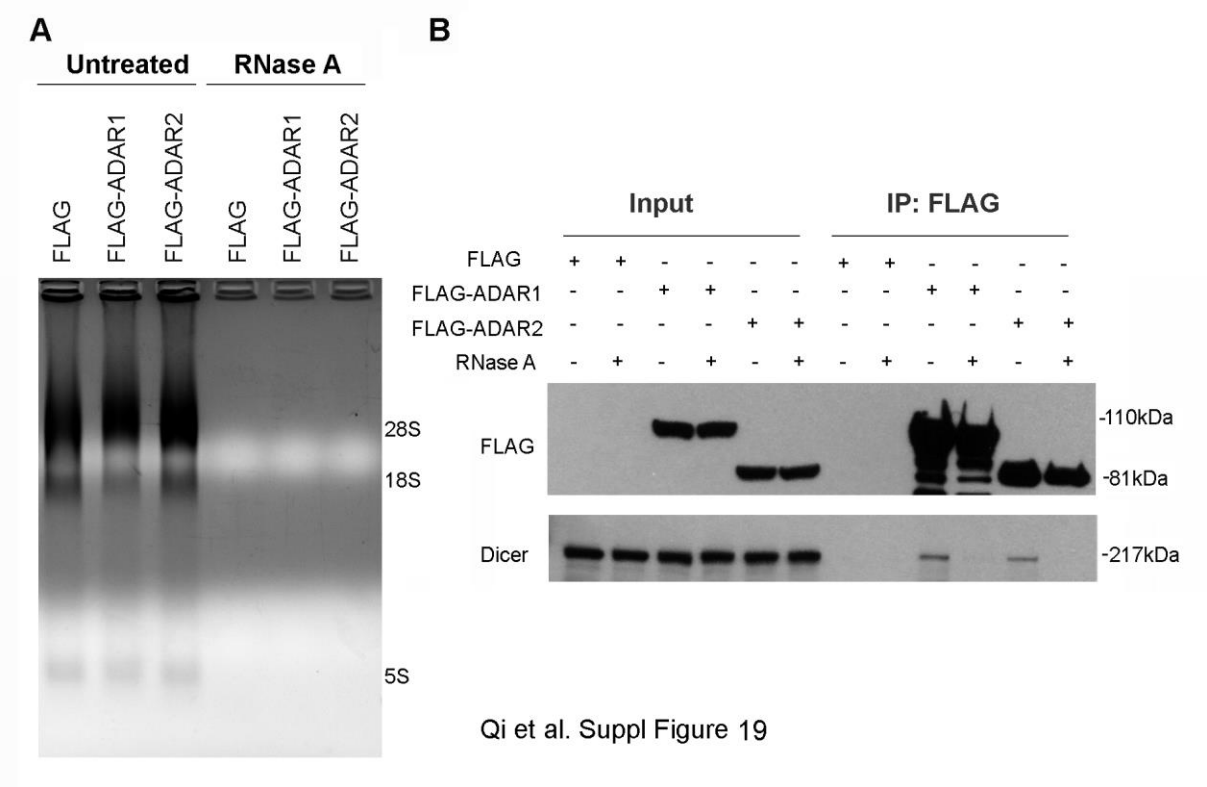

Figure S19. Interaction between ADARs and Dicer may be mediated by RNA molecules. (**A, B**) Total lysates of HEK293T cells overexpressing FLAG only or FLAG-tagged ADAR1/2 were treated without (untreated) or with RNase A (1ug/mL) for 30 minutes at 37˚C. Complete degradation of RNAs was confirmed by running 1% agarose gel electrophoresis (**A**), followed by the immunoprecipitation (**B**) using anti-FLAG antibody conjugated magnetic beads (IP: FLAG). Western blot analyses of the indicated proteins in 5% of total lysates (Input) and FLAG-IP products were conducted.

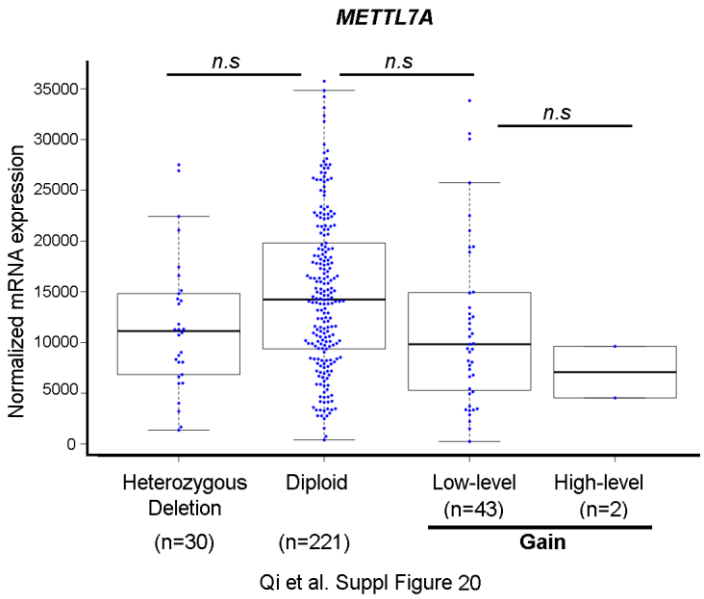

Figure S20. The downregulation of METTL7A is not associated with the genomic loss of *METTL7A* gene. Copy number variation and mRNA expression analyses of the *METTL7A* gene of TCGA datasets showed the mRNA expression level of METTL7A was not correlated with the copy number change in 296 HCC patients. *n.s*, no significance; Mann-Whitney U test.

Supplementary Table S1. List of selected target genes with multiple editing sites at 3'UTRs

Gene ID	3'UTR length	No. of editing sites [α]	Functions
CCNYL1 (cyclin Y like 1)	2,474 bp	3	its paralog gene CCNY is highly similar to cyclin B3, and able to activate c-Myc transcriptional activities(6)
TNFAIP8L1 (Tumor Necrosis Factor, Alpha-Induced Protein 8-Like 1)	3,138 bp	2	also known as TIPE1, highly expressed in human carcinoma cell lines, especially viral DNA transformed cell line (7)
MDM2 (Mouse double minute 2 homolog)	5,583 bp	5	Negative regulator of p53 which is a critical tumor suppressor, and mutated (or inactive) in most human cancers(8)
METTL7A (Methyltransferase Like 7A)	2,367 bp	13	Also known as AAM-B, targeted to lipid droplet, predicted to be a methyltransferase based on sequence homology(9)
MTDH (Metadherin)	5,590 bp	4	Also known as AEG-1 or LYRIC, amplified and over-expressed in HCC. High expression of MTDH correlates with tumor aggressiveness(10)
RBBP9 (retinoblastoma binding protein 9)	3,220 bp	3	Identified as Bog gene expressed in transformed rat liver epithelial cell lines resistant to TGFβ inhibitory effects (11). It was also demonstrated to be involved in pancreatic carcinomas through its elevated serine hydrolase activity (12).

[α] Number of editing sites present in at least 2 out of 3 patients identified from our previously published RNA-Seq datasets(2,13)

Supplementary Table S2. Sequences of primers used for cloning 3'UTRs of selected genes

Primer name	Primer sequence (5'-3') [α]
CCNYL1-3'UTR- SacI-F	CCTTGAGCTCAAGGAGAAATGAGGGGTTATA
CCNYL1-3'UTR- NheI-R	AATTGCTAGCTTAATTAAAATAGAGTTTATTAGCTTTTAA
TNFAIP8L1-3'UTR- SacI-F	CCTTGAGCTCACCCCGGCGCCGCCCAACCGC
TNFAIP8L1-3'UTR- NheI-R	AATTGCTAGCCCCAGGCTGGTGTGTGCTTTTAT
MDM2-3'UTR- SpeI-F	CCTTACTAGTTTGACCTGTCTATAAGAGAATTATA
MDM2-3'UTR- XhoI-R	CCTTCTCGAGTGCTTGCTTTACGGTTTTATTTTGC
METTL7A-3'UTR- SacI-F	CCTTGAGCTCAATTTTTTTTCCTGAATTGGACATG
METTL7A-3'UTR- NheI-R	AATTGCTAGCTAAACCATATTTCTGTTCCTAAC
MTDH-3'UTR- SacI-F	CCTTGAGCTCAATTTTTTTTCCTGAATTGGACATG
MTDH -3'UTR- NheI-R	AATTGCTAGCTGGTGGTTTCAGATGTGTTCATT
RBBP9-3'UTR- SpmeI-F	ATATGTTTAAACACTGTATGATTTCTGCTATTTTGC
RBBP9-3'UTR- XhoI-R	ATATCTCGAGTTCCCATGGTATGTTTTTAATTC
METTL7A-3'UTRMut-F	GTTCTTTGCAACTATGGAAGGACACTTAATCA TCACAAGTGCCTCTG
METTL7A-3'UTRMut-R	CAGAGGCACTTGTGATGATTAAGTGTCCTTCC ATAGTTGCAAAGAAC
METTL7A-ΔAlu Mut-F	AAAAAGAGACAGGGGTAGAGACA
METTL7A--ΔAlu Mut-R	TCTCCCTGTCTCTACCCCT

[α] Restriction enzyme sites incorporated into the primers are underlined.

Supplementary Table S3. Sequences of primers used for analysing editing sites of selected 3'UTRs and miRNAs

Primer name	Primer sequence (5'-3')
MPHOSPH8-3'UTR- ed-F	CCACAATGTGGATAGTACATATG
MPHOSPH8-3'UTR- ed-R	GCTGACAGCCAGGTTTGGCTGTT
CCNYL1-3'UTR- ed-F	CACTGCAGCATGAGTATAAATG
CCNYL1-3'UTR- ed-R	GGGTACTGAGATTACAGGCATGA
TNFAIP8L1-3'UTR- ed-F1	CCTGTAATCCCAGCACTTTGAGAG
TNFAIP8L1-3'UTR- ed-R1	CTTCCCTCGTCATCTCTC
TNFAIP8L1-3'UTR- ed-F2	GAGGGGAAACTGCTCCAATC
TNFAIP8L1-3'UTR- ed-R2	GGTTGCTGATTCTCCAAATATGA
METTL7A-3'UTR- ed-F	GGGAAGAAAGAGTTTTGCTCTTG
METTL7A-3'UTR- ed-R	TGGGAGACAATAGAAAATGGCTA
RBBP9-3'UTR- ed-F	CCTCCCAAGTAGTGTGAACTAAAG
RBBP9-3'UTR- ed-R	GGATAAAGTAAAATAAGGGGCCG
hsa-miR-27a-ed-F	CTGAGCTCTGCCACCGAGGAT
hsa-miR-27a-ed-R	AGGCAGCAGGATGGCAGGCA

Supplementary Table S4. Sequences of primers used to clone wild type and mutant ADARs into pLenti6 lentiviral expression vector.

Primer name	Primer sequence (5'-3')
ADAR1-p110-BamHI-F	TCTCGGATCCATGGCCGAGATCAAGGAGAAAATCT
ADAR1-p110-XhoI-R	TCTCCTCGAGCTATACTGGGCAGAGATAAAAGTTC
ADAR2-BamH1-F	TTAAAGATCTATGGATATAGAAGATGAAGAAAAC
ADAR2-XhoI-R	TTAAGTCGACTCAGGGCGTGAGTGAGAACTGG
ADAR1-EAA-F1	GCTGAAGCTGGAAGCGAGGCCGTGGCGGCGCAGGATGCAGCTATGAAAGC
ADAR1-EAA-R1	GCTTTCATAGCTGCATCCTGCGCCGCCACGGCCTCGCTTCCAGCTTCAGC
ADAR1-EAA-F2	CCAGTGTGAGTGCACCCAGCGAGGCAGTGGCAGCGCAGATGGCCGCAGAGG
ADAR1-EAA-R2	CCTCTGCGGCCATCTGCGCTGCCACTGCCTCGCTGGGTGCACTCACACTGG
ADAR1-EAA-F3	CGTCTGCGCACACAGCGAGGCCCAAGGGGCGCAGGAAGCAGCAGATGC
ADAR1-EAA-R3	GCATCTGCTGCTTCCTGCGCCCCTTGGGCCTCGCTGTGTGCGCAGACG
ADAR2-EAA-F1	GGCTCTGGTCCCACAGAGGCAAAGGCAGCACTGCATGCTGCTGAGAAGG
ADAR2-EAA-R1	CCTTCTCAGCAGCATGCAGTGCTGCCTTTGCCTCTGTGGGACCAGAGCC
ADAR2-EAA-F2	GGCTCGGGGAGAAACGAGGCGCTTGCCGCGGCCCGGGCTGCGC
ADAR2-EAA-R2	GCGCAGCCCGGGCCGCGGCAAGCGCCTCGTTTCTCCCCGAGCC
ADAR1-DeAD-F	GAGAAACTGTCAATGACTGCTATGCAGCAATAATCTCCCGGAGAGGCTT
ADAR1-DeAD-R	AAGCCTCTCCGGGAGATTATTGCTGCATAGCAGTCATTGACAGTTTCTC
ADAR2-DeAD-F	CATTAAATGACTGCCATGCAGCAATAATATCTCGGAGATCCTT
ADAR2-DeAD-R	AAGGATCTCCGAGATATTATTGCTGCATGGCAGTCATTTAATG

Supplementary Table 5. Sequences of primers used to construct shRNAs against *ADARs* and *METTL7A*.

Primer name	Primer sequence (5'-3')
shADAR1-aF	CCGGAGTTTCCTGCTTAAGCAAATACTCGAGTATTTGCTTAAGCAGGAAACTTTTTTG
shADAR1-aR	AATTCAAAAAAGTTTCCTGCTTAAGCAAATACTCGAGTATTTGCTTAAGCAGGAAACT
shADAR1-bF	CCGGATCAGGAACAAAGGATCTTAACTCGAGTTAAGATCCTTTGTTCCTGATTTTTTG
shADAR1-bR	AATTCAAAAAATCAGGAACAAAGGATCTTAACTCGAGTTAAGATCCTTTGTTCCTGAT
shADAR2-a (TRCN0000050939)	CCGGCCCGTGATGATCTTGAACGAACTCGAGTTCGTTCAAGATCATCACGGGTTTTTG
shADAR2-b (TRCN0000050942)	CCGGCCCAGGACTCAAGTATGACTTCTCGAGAAGTCATACTTGAGTCCTGGGTTTTTG
shMETTL7A_aF	CCGGATAGTGTGAGCTGGCAGTTAACTCGAGTTAACTGCCAGCTCACACTATTTTTTG
shMETTL7A_aR	AATTCAAAAAATAGTGTGAGCTGGCAGTTAACTCGAGTTAACTGCCAGCTCACACTAT
shMETTL7A_bF	CCGGCTGAATGGCTCAAAGAATTTACTCGAGTAAATTCTTTGAGCCATTCAGTTTTTG
shMETTL7A_bR	AATTCAAAAACTGAATGGCTCAAAGAATTTACTCGAGTAAATTCTTTGAGCCATTCAG
shMETTL7A_cF	CCGGTGGTGAGGTTCACTGTGATATCTCGAGATATCACAGTGAACCTCACCATTTTTG
shMETTL7A_cR	AATTCAAAAATGGTGAGGTTCACTGTGATATCTCGAGATATCACAGTGAACCTCACCA

Supplementary Table S6. Sequences of primers used for cloning miRNA precursors

Primer name	Primer sequence (5'-3') [α]
hsa-miR-93-F	TTAAGAATTCACTACATCACAGCAGCATACGTG
hsa-miR-93-R	TTAAGCGGCCGCGTGCCTAAGGGGAAGGTAGG
hsa-miR-93 scr-F[b]	AGTGTGATTACCCAACCT*GTACTATTGATCCAGACC*CCAGAGCCCCCGGGA CACGTTCT
hsa-miR-93 scr-R	ACAGGTTGGGTAATCACACTGTTACTCATTGACCAGACCGCGAGCCCCCA GGACTGAGGTC
hsa-miR-612-F	TTAAGAATTCTCTGCTGCTGCAGTAAGTAAGTG
hsa-miR-612-R	TTAAGCGGCCGCCTTCCATTCTCTGATCTGTCAGC
hsa-miR-17-F	TTAACAATTGGTATTTGCTAAGTGGAAGCCAGA
hsa-miR-17-R	TTAAGCGGCCGCAATAGCAGGCCACCATCAGT
hsa-miR-940-F	TTAAGAATTCCATGTCTGAGGAGTGGGTATCAT
hsa-miR-940-R	TTAAGCGGCCGCACTGCAGTCACTTAGGCTGCTC
hsa-miR-20b-F	TTAAGAATTCCAGTGCAGGTAGCTTTTTGAGAT
hsa-miR-20b-R	TTAAGCGGCCGCCCTGCGGTTTACAGATGGAT
hsa-miR-654-F[c]	CACCATCAGGGAAGAGACAATAA
hsa-miR-654-R	TTAAGCGGCCGCACCCCGTTCATTCAGATACG
hsa-miR-93-F	TTAAGAATTCACTACATCACAGCAGCATACGTG
hsa-miR-93-R	TTAAGCGGCCGCGTGCCTAAGGGGAAGGTAGG
hsa-miR-610-F	TTAAGAATTCAATTGGAGTCCCAGAAGTAGAGG
hsa-miR-610-R	TTAAGCGGCCGCGACAGAGTTTCACCATGTTAGCC
hsa-miR-637-F	TTAAGAATTCTAAAGTGCCAGAGGTGGTTAGAC
hsa-miR-637-R	TTAAGCGGCCGCCTGGTGTTGCTGAAGTACTCCTC
hsa-miR-27a-F	ATATGAATTCCTGAGCTCTGCCACCGAGGAT
hsa-miR-27a-R	ATATGCGGCCGCAGGCAGCAGGATGGCAGGCA

[α], Underlined letters indicate the EcoRI and NotI restriction enzyme recognition sites introduced for cloning

[b], For the scrambled control, mature miR-93 seed sequence is scrambled, as shown by the italic letters

[c], No need to introduce EcoRI site into hsa-miR-654-F primer as an intrinsic EcoRI site exits in the 1000-bp PCR fragment

Supplementary Table S7. Sequences of primers used for qRT-PCR

Primer name	Primer sequence (5'-3')
ADAR1-qRT-F	GCTGAAGCTGGAAGCAAGAAAGTG
ADAR1-qRT-R	CAGGGCCTTCTTTGGACAGGA
ADAR2-qRT-F	CTGACACGCTCTTCAATGGTT
ADAR2-qRT-R	GGCGCAGTTCGTTCAAGAT
METTL7A-qRT-F	GGGAAGAAAGAGTTTTGCTCTTG
METTL7A-qRT-R	TGGGAGACAATAGAAAATGGCTA
miR-27a-premiRNA-F	CAGGGCTTAGCTGCTTGTGA
miR-27a-premiRNA-R	GCGGAACTTAGCCACTGTGA
pri-miRNA-qF	CTCCCCAGTAGAGCTGGGACTA
pri-miRNA-qR	TCACACCTGAGCCACCTGTAAT
pre-miR-27a-probe	TCC ACA CCA AGT C

SUPPLEMENTARY REFERENCES

1. Peng, Z., Cheng, Y., Tan, B.C., Kang, L., Tian, Z., Zhu, Y., Zhang, W., Liang, Y., Hu, X., Tan, X. *et al.* (2012) Comprehensive analysis of RNA-Seq data reveals extensive RNA editing in a human transcriptome. *Nat Biotechnol*, **30**, 253-260.
2. Chan, T.H., Lin, C.H., Qi, L., Fei, J., Li, Y., Yong, K.J., Liu, M., Song, Y., Chow, R.K., Ng, V.H. *et al.* (2014) A disrupted RNA editing balance mediated by ADARs (Adenosine DeAminases that act on RNA) in human hepatocellular carcinoma. *Gut*, **63**, 832-843.
3. Lai, F., Drakas, R. and Nishikura, K. (1995) Mutagenic analysis of double-stranded RNA adenosine deaminase, a candidate enzyme for RNA editing of glutamate-gated ion channel transcripts. *J Biol Chem*, **270**, 17098-17105.
4. Valente, L. and Nishikura, K. (2007) RNA binding-independent dimerization of adenosine deaminases acting on RNA and dominant negative effects of nonfunctional subunits on dimer functions. *J Biol Chem*, **282**, 16054-16061.
5. Sato, K., Hamada, M., Asai, K. and Mituyama, T. (2009) CENTROIDFOLD: a web server for RNA secondary structure prediction. *Nucleic Acids Res*, **37**, W277-280.
6. Yang, W., Chendrimada, T.P., Wang, Q., Higuchi, M., Seeburg, P.H., Shiekhattar, R. and Nishikura, K. (2006) Modulation of microRNA processing and expression through RNA editing by ADAR deaminases. *Nat Struct Mol Biol*, **13**, 13-21.
7. Cui, J., Zhang, G., Hao, C., Wang, Y., Lou, Y., Zhang, W., Wang, J. and Liu, S. (2011) The expression of TIPE1 in murine tissues and human cell lines. *Mol Immunol*, **48**, 1548-1555.
8. Wade, M., Li, Y.C. and Wahl, G.M. (2013) MDM2, MDMX and p53 in oncogenesis and cancer therapy. *Nat Rev Cancer*, **13**, 83-96.
9. Zehmer, J.K., Bartz, R., Liu, P. and Anderson, R.G. (2008) Identification of a novel N-terminal hydrophobic sequence that targets proteins to lipid droplets. *J Cell Sci*, **121**, 1852-1860.
10. Sarkar, D. (2013) AEG-1/MTDH/LYRIC in liver cancer. *Adv Cancer Res*, **120**, 193-221.
11. Woitach, J.T., Zhang, M., Niu, C.H. and Thorgeirsson, S.S. (1998) A retinoblastoma-binding protein that affects cell-cycle control and confers transforming ability. *Nat Genet*, **19**, 371-374.
12. Shields, D.J., Niessen, S., Murphy, E.A., Mielgo, A., Desgrosellier, J.S., Lau, S.K., Barnes, L.A., Lesperance, J., Bouvet, M., Tarin, D. *et al.* (2010) RBBP9: a tumor-associated serine hydrolase activity required for pancreatic neoplasia. *Proc Natl Acad Sci U S A*, **107**, 2189-2194.
13. Chen, L., Li, Y., Lin, C.H., Chan, T.H., Chow, R.K., Song, Y., Liu, M., Yuan, Y.F., Fu, L., Kong, K.L. *et al.* (2013) Recoding RNA editing of AZIN1 predisposes to hepatocellular carcinoma. *Nat Med*, **19**, 209-216.